ELSEVIER SAUNDERS

NEUROIMAGING CLINICS OF NORTH AMERICA

Neuroimag Clin N Am 16 (2006) 149–167

Pediatric Perfusion MR Imaging Using Arterial Spin Labeling

Jiongjiong Wang, PhD[a,*], Daniel J. Licht, MD[b]

Significant gaps exist in our knowledge of pediatric cerebral blood flow (CBF) and its relation to the timing and cause of brain injury, despite a growing wealth of literature on the relation and significance of structural brain MR imaging data and neurocognitive development [1–4]. Pediatric stroke and perinatal hypoxic-ischemic encephalopathy (HIE) are two prominent examples where valuable knowledge in cerebral perfusion is lacking.

CBF (cerebral perfusion) mirrors cerebral metabolic demand and neuronal function, and therefore, is a vital parameter in the evaluation of pediatric brain injury and recovery. Until recently, measurement of CBF involved intravenous bolus injection of contrast agents or nuclear medicine methods that were technically difficult or ethically problematic in pediatrics. The development of arterial spin label (ASL) perfusion MR imaging as a noninvasive method for measuring CBF allows for the increased ability to measure this vital physiologic parameter in any age group. This article presents the technical aspects of performing ASL perfusion MR imaging in pediatrics, and discusses its current use in clinical studies and its potential in influencing important management strategies for specific disease entities.

Methodologic background

The dynamic susceptibility contrast (DSC) approach remains the primary MR imaging method to assess cerebral hemodynamics, although its application in children has been less widespread than in adults [5,6]. DSC MR imaging captures the first passage of a susceptibility contrast agent, such as gadolinium–diethyltriaminepentaacetic acid (Gd-DTPA), through the cerebral vasculature. Multiple hemodynamic parameters, including CBF,

This work was supported by the Thrasher Research Fund, National Institutes of Health Human Brain Project (R21 MH072576, HD049893, and NS052380), Pfizer Scholarship, and the W.W. Smith Charitable Trust.

[a] Department of Radiology, University of Pennsylvania, Philadelphia, PA, USA
[b] Division of Neurology, Children's Hospital of Philadelphia, Philadelphia, PA, USA
* Corresponding author. Department of Radiology, University of Pennsylvania, 3400 Spruce Street, Philadelphia, PA 19104.
E-mail address: wangj3@mail.med.upenn.edu (J. Wang).

1052-5149/06/$ – see front matter
doi:10.1016/j.nic.2005.10.002
neuroimaging.theclinics.com

cerebral blood volume (CBV), and mean transit time (MTT), can be estimated from temporal characteristics of the first-pass time course [7]. Although these parameters are, in general, relative, in many clinical cases they are indicative of regional pathologic changes in hemodynamics. Another advantage of DSC is that the susceptibility contrast agent causes a large change in MR imaging signal (20%–50%, depending on the dosage, imaging sequence, and magnetic field strength), which renders a high signal-to-noise ratio (SNR) and reliability in clinical diagnoses. The disadvantage of DSC is the requirement of an intravenous catheter for power or manual injection of contrast agent, which may be technically difficult in small children and infants. DSC measurements cannot be repeated during a single scanning session because of cumulative effects, and comparison between multiple scans in a longitudinal study is difficult without absolute quantification. The article by Cha elsewhere in this issue explains DSC perfusion imaging in greater depth.

ASL perfusion MR imaging is an alternative and emerging noninvasive method to measure CBF directly by using magnetically labeled arterial blood water as an endogenous contrast agent (tracer) [8,9]. Its methodologic scheme is analogous to that used in positron emission tomography (PET) and single-photon emission CT (SPECT) [10]. Arterial blood water is magnetically labeled through inversion or saturation proximal to the tissue of interest, and image acquisition usually is performed after a delay time that allows the labeled blood to flow into the imaging slices. Perfusion can be determined by pair-wise comparison with separate images that are acquired without labeling (control). Repeated measurements of interleaved label and control acquisitions are performed to improve the SNR of perfusion images, which often requires a few minutes of scan time. By taking into account the tracer decay rate of T1, absolute CBF can be quantified in well-characterized physiologic units of mL/100 g/min. Because ASL does not require administration of contrast agent or radioactive tracer, it is much safer, more economical, and convenient compared with existing radioactive and dynamic contrast MR approaches. The improved safety of ASL, without the need for intravenous injection, is particularly appealing for the pediatric population, and allows perfusion imaging in a wide range of age groups from adolescents to neonates. Additionally, ASL scans can be repeated as often as required during the same scanning session without cumulative effects.

During the past decade, theoretic and experimental studies have been performed to improve the accuracy of CBF quantification using ASL by taking into account multiple parameters, such as arterial transit time [11–15], magnetization transfer effect [14,16,17], T1 [18,19], labeling efficiency [20–22], and capillary water permeability [23–25]. CBF measurements with ASL perfusion MR imaging recently were shown to agree with results from ^{15}O-PET [26] and the DSC approach [27,28]. ASL perfusion measurements at rest and during task activation were demonstrated to be highly reproducible across intervals that varied from a few minutes to a few days [29,30]. In clinical applications, ASL also is a valuable tool in various neurologic and psychiatric disorders in adults [31–34]. The primary weakness of ASL, as compared with DSC MR imaging, is the small labeling effect (< 1% raw signal) [8,9]. This limitation arises from the fact that the volume of arterial blood that is available for labeling is only on the order of 1% to 2% of total brain volume. The labeled blood further relaxes during the transit from the labeling region to the brain, which results in a net labeling effect of less than 1% of raw MR imaging signal in brain tissue. Because the arterial transit time from the labeling region to the brain is comparable to the tracer decay rate that is determined by the T1 of blood, ASL technique is sensitive to transit effects, and often results in focal intravascular signal in perfusion images.

Aspects of pediatric physiology provide a natural solution to overcoming the two limitations of ASL (low SNR and transit effect). First, normally increased blood flow in children [35] provides improved ASL perfusion contrast as compared with adult studies. Previous evidence also suggested that the water content of brain is higher in children than in adults [36]. This results in increased equilibrium MR signal and spin-lattice, spin-spin relaxation time (T1, T2), and thereby, improves pediatric ASL signal through increased tracer concentration and lifetime. Second, data from Doppler ultrasound studies suggest that blood flow velocities in carotid arteries are higher in healthy children compared with adults, with the peak velocity during the age range of 5 to 8 years [37]. This effect can be translated into normally reduced arterial transit time for labeled blood to flow from the labeling region to the brain, which results in reduced relaxation of the labeling effect and reduced transit effect (focal intravascular signal) in pediatric perfusion images. In a feasibility study at 1.5 T, we observed that brain T1 and proton density image intensity (M0), and thereby, the SNR of ASL perfusion images, decrease linearly with age. On average, a 70% improvement in the SNR of perfusion images was observed in neurologically normal children as compared with healthy adults [38]. **Fig. 1** clearly demonstrates prolonged brain T1 in children as compared with adults. The representative child

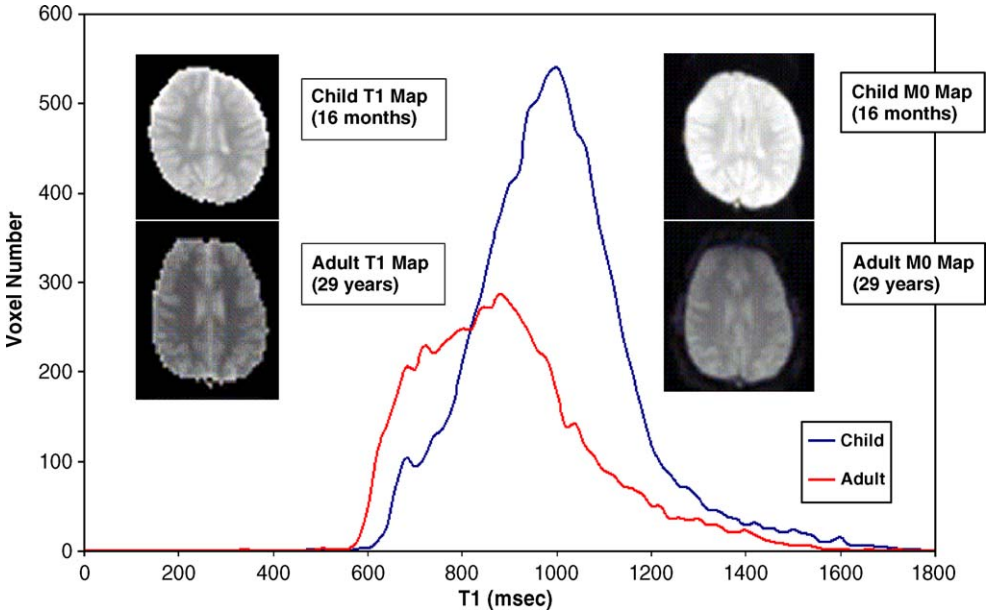

Fig. 1. T1 line graph averaged across seven children and five adults with representative T1 and M_0 images acquired in a 16-month-old child and 29-year-old adult (displayed using same scale). The child T1 and M_0 images have higher intensities than do the adult images.

M0 image also is much brighter than adult M0 images because of increased water content. Fig. 2 displays four representative sets of pulsed ASL (PASL) perfusion images that were acquired at three delay times in three children (a–c) and one adult (d) at 1.5 T. Pediatric perfusion images provide much stronger perfusion signal and improved delineation of cortical and subcortical structures compared with adult perfusion images. Given the unique and reciprocal benefits in terms of safety and image quality, ASL methods may be ideally suited for pediatric perfusion imaging.

Continuous versus pulsed arterial spin labeling

ASL techniques can be divided generally into two categories: continuous ASL (CASL) and PASL. In CASL, a labeling plane is applied at the base of the brain for 1 to 2 seconds, during which arterial blood that is flowing through the plane is magnetically tagged (inverted). In PASL, a thick slab of blood inferior to the imaging slices is inverted instantly using radiofrequency (RF) pulses with high peak amplitude, but short duration (10–20 milliseconds). Although CASL provides stronger perfusion contrast, it is more challenging for implementation and deposits a higher level of RF power into the subject compared with PASL. The long labeling pulses in CASL also partially excite the imaging slices through an effect that is termed magnetization transfer. This has to be balanced during the control acquisitions to quantify CBF accurately. Conversely, PASL methods require a well-designed slice profile for the labeling pulse with a sharp edge to eliminate residual signal from static tissue.

Because of the technical simplicity and low RF power level, initial testing in the pediatric population was performed using a PASL method at 1.5 T. The PASL method was modified from the flow sensitive alternating inversion recovery (FAIR) technique [39] by applying a saturation pulse at a certain time point after the labeling pulse to externally define the tagging bolus duration [19]. Although feasibility has been demonstrated in children of various ages, the authors encountered a few technical challenges. As displayed in Fig. 3, the FAIR technique uses a spatially extended inversion band for arterial labeling, especially in combination with the body transmitter coil. In adults, the inversion band primarily covers the carotid arteries, whereas in the infant it covers the upper thorax and beyond. Although the total magnetization of the labeled blood may be increased, this labeling scheme may not be optimal because of uncertainties in the labeled arterial blood volume. For instance, because the blood flow velocity is fast in normal children, labeled arterial blood in the systemic circulation may reach the brain before being spoiled by the saturation pulse; this causes a larger than expected tagging bolus, and thereby, an overestimation of blood flow. In neonates who have

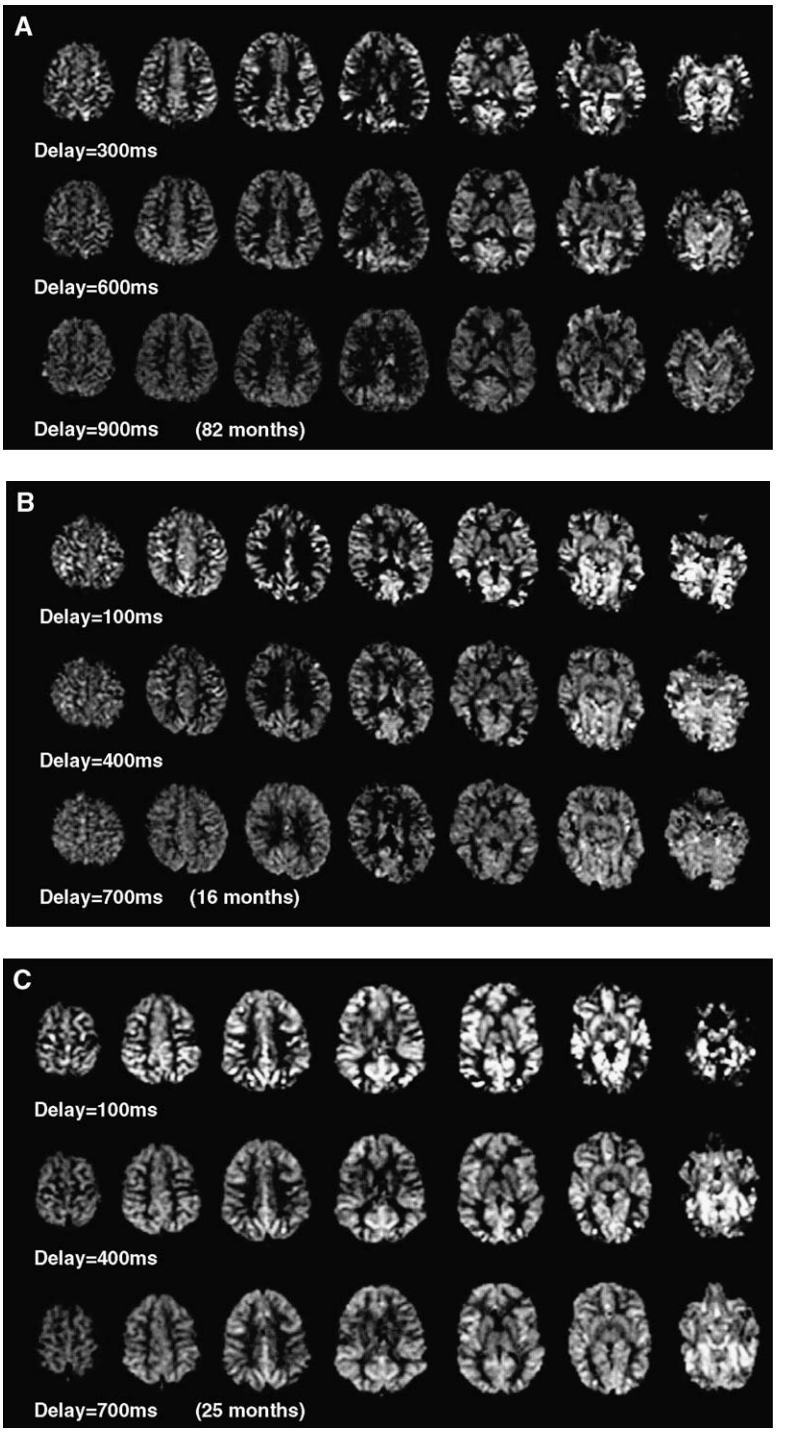

Fig. 2. Four representative sets of PASL perfusion images acquired at three delays in three children (*A–C*) and one adult (*D*) at 1.5 T.

congenital heart defects (CHDs), blood flow is extremely low, whereas the tracer lifetime (blood T1) is long [40]. A considerable amount of labeled blood from the systemic circulation will not be spoiled by the saturation pulse and flows into the brain tissue when the subsequent (control) acquisition is performed. This may lead to cross-contamination of the label and control acquisitions and a negative signal in the resultant perfusion images. The mixing (intra- and extracardiac shunts)

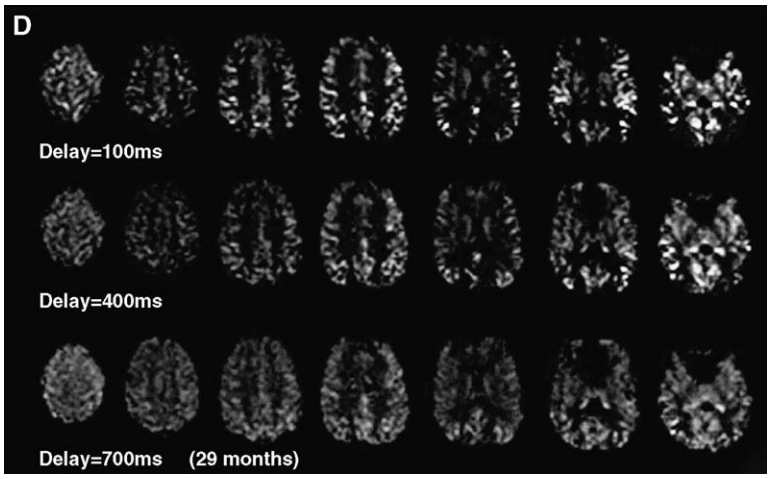

Fig. 2 (*continued*).

of blood between the pulmonary and systemic circulations in infants who have CHDs also may be a factor, because the labeled blood from the body may have a shorter transit to the brain. The authors observed negative perfusion values in an average of 40% of brain pixels in neonates who had severe CHDs. When the labeling slab was restricted spatially to exclude systemic circulation [see Fig. 3C], the number of pixels with negative values and the intersubject variability of perfusion measurements were reduced [41]. These observations suggest that a well-defined, or even tailored tagging slab, in conjunction with effective spoiling saturation pulses for PASL perfusion imaging, is necessary in children who have different ages (particularly infants) or diseases.

In contrast, the CASL method uses a thin labeling plane proximal to the tissue of interest, and therefore, is not sensitive to the effect of the tagging slab as in PASL. Furthermore, CASL offers an improved SNR over PASL. In the past, the use of CASL in children has been limited by the safety concern of the high level of RF power. Theoretic and experimental data showed that the specific absorption rate (SAR) of RF power is roughly proportional to the square of the head size (radius) [42,43], which results in a lower SAR level in children compared with adults. CASL methods generally use the strategy of flow-driven adiabatic inversion, which has an optimal flow velocity range to reach the theoretic tagging efficiency. Although existing CASL applications in children followed parameters that were derived from adults, optimization and simulation may need to be performed for pediatric perfusion imaging, because the variability of flow velocities in children may be large. Another issue that is related to CASL is that not all commercial MR imaging scanners allow long (a few seconds) RF pulses for labeling, and many vendors set a limit on the duty cycle for the RF amplifier. Nevertheless, multislice CASL recently was implemented successfully on the MR imaging scanners of several major vendors, although complete commercialization may take years.

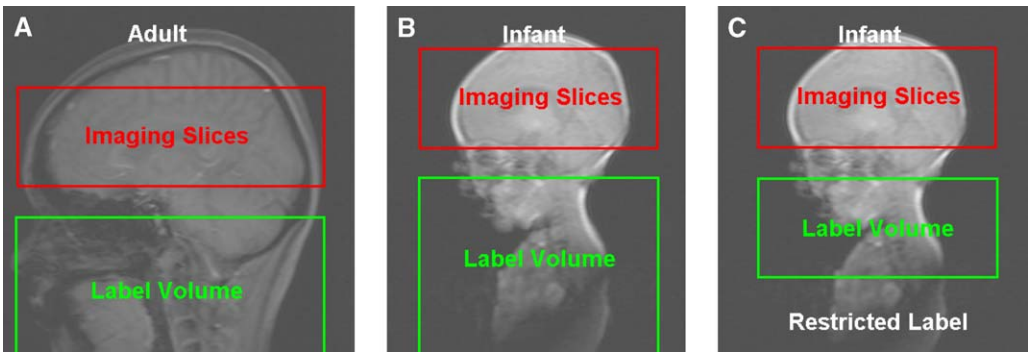

Fig. 3. Diagram showing the labeling scheme of the PASL method in adult (*A*) and infant (*B*), and the modified PASL method with restricted label volume in infant (*C*).

High versus low magnetic field

The low SNR is the primary limitation that hampers the widespread application of ASL perfusion MR imaging. Performing ASL at a high magnetic field offers a natural solution to improve the image quality and to reduce transit-related effects [18]. SNR is proportional to the main field strength, and there is an improved labeling effect because of prolonged tracer lifetime (T1) at a high field. Because of the shortened T2/T2*, the net SNR gain in high-field ASL is compromised, as shown in Fig. 4A, which demonstrates the theoretic calculation of PASL and CASL signals as a function of the static field strength. As shown, a twofold signal gain is readily achievable by performing PASL at 3.0 T and 4.0 T, as compared with PASL methods at 1.5 T [18,44]. This allows improved spatiotemporal resolution and longer postlabeling delay times to counteract delayed transit effects that usually are present in a patient population. The implementation of CASL at a high magnetic field is expected to provide even greater perfusion contrast and SNR gain (more than threefold) than PASL methods [18].

Two important challenges for using continuous labeling are controlling for the off-resonance effects

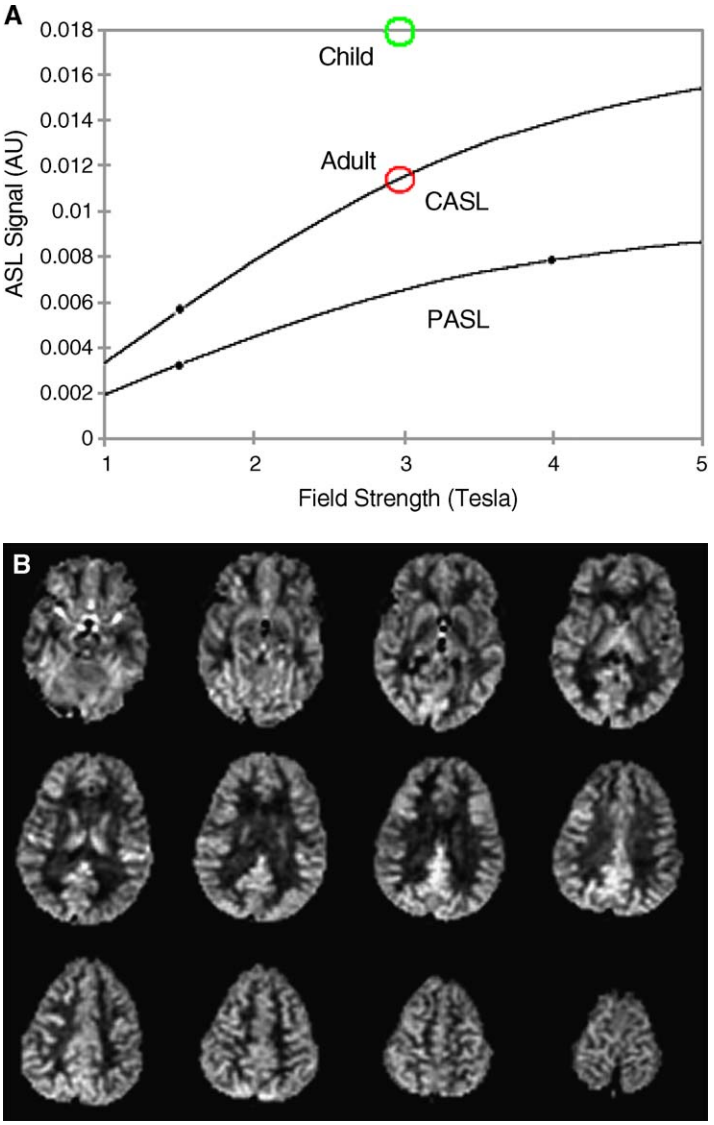

Fig. 4. (*A*) Theoretic ASL signal as a function of field strength. The black circles indicate the conditions for the experimental data that were reported in reference 18; the red and green circles indicate the 3.0-T CASL signals in adults and children, respectively. (*B*) Representative child (8-year-old boy) perfusion images acquired using AM CASL at 3 T, showing image quality approaching routine structural MR imaging.

that are caused by RF irradiation (magnetization transfer effect) and achieving ample labeling efficiency within the safety constraints for RF power deposition. Recently, two approaches have been performed successfully for the implementation of CASL at 3.0 T: the use of separate small RF coils for labeling of carotid arteries [45,46] and the use of amplitude-modulated (AM) control pulses to mimic the off-resonance effect of the labeling pulse [47,48]. Although the total RF power is lower in the dual-coil approach, it requires special hardware that may limit its application in clinical settings. For AM CASL, the amplitude of the labeling pulses has to be reduced to keep the power of RF irradiation within the SAR limitation at 3.0 T. Optimal perfusion contrast can be achieved by keeping the magnitudes of the labeling pulses and gradients in proportion (simultaneously reduced). Experimental data demonstrated a 30% to 40% improvement in SNR using AM CASL, compared with PASL, at 3.0 T [48]. The advantage of this AM CASL approach is that high-quality perfusion images with whole-brain coverage can be obtained within a few minutes using standard clinical MR hardware. The benefit of high-field CASL, in conjunction with the natural ASL signal gains in children, yield impressive pediatric perfusion images at 3.0 T, the quality of which approaches that of routine anatomic MR scans [Fig. 4B]. Because 3-T MR imaging scanners are becoming available at many neuroimaging centers, high-field CASL is expected to have widespread applications, particularly in the pediatric population.

Multicontrast hemodynamic neuroimaging using arterial spin labeling

DSC MR imaging is capable of providing estimations of multiple hemodynamic parameters, including CBF, CBV, MTT, and time-to-peak. Although these parameters are related through the central volume principle, each represents a different aspect of cerebral circulation, and has a specific meaning in clinical use, especially in combination with other parameters. ASL methods, in contrast, generally provide a single estimation of CBF. Transit-related effect is the major confounding factor that affects the accuracy of perfusion measurements using ASL; however, the measurement of arterial transit time itself is clinically significant, because it may indicate collateral sources of blood supply in cerebrovascular disease. Recent technical developments have demonstrated that arterial transit time—the duration for the labeled blood to flow from just below the circle of Willis to the brain tissue—can be imaged using the flow-encoding arterial spin tagging (FEAST) technique [49]. This method uses appropriate bipolar gradients to differentiate the ASL signals in the vascular and microvascular compartments. The ratio of these two quantities yields an estimation of transit time, because more labeled blood water enters the micro-

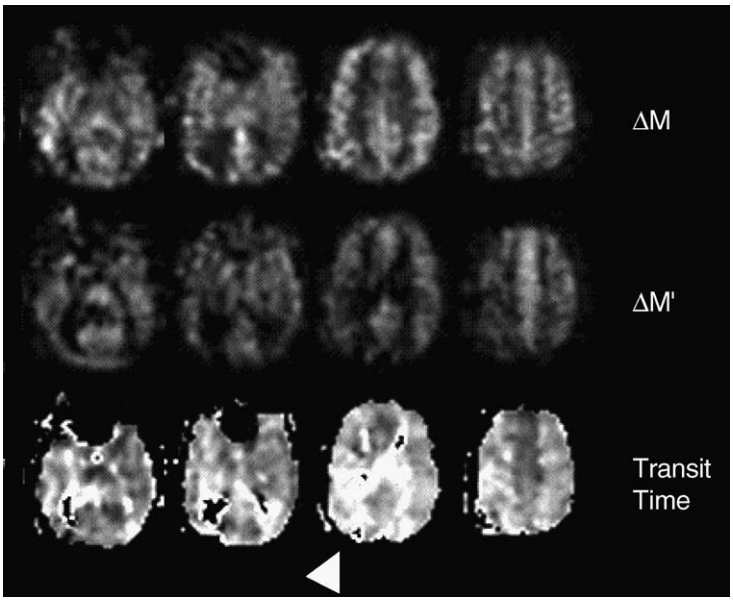

Fig. 5. An example of the processing steps for FEAST transit time measurement of an adult patient (37-year-old woman) who had right middle cerebral artery (MCA) stenosis. The upper two panels are ASL images acquired without (ΔM) and with (ΔM') gradients, respectively. Transit time images (*bottom panel*) are calculated from the ratio of the two measurements that display prolonged transit time in posterior right MCA district (*arrow*).

vascular compartment with shorter transit time and vice versa [Fig. 5]. The significance of transit time measurement is that it can detect (correct) transit-related artifact in ASL perfusion images and provide additional information regarding collateral blood supply. Because of the autoregulation effect, normal perfusion can be maintained in the presence of decreasing arterial pressure until the vascular reserve is exhausted. Conversely, transit time is more sensitive to, and generally follows, the change in arterial pressure. The combination of transit time and perfusion measurements provides the potential to grade the status of cerebral hemodynamic impairment into two stages of "hemodynamic compromise" and "misery perfusion" [50]. This information is expected to improve accuracy in the diagnosis of childhood cerebrovascular disease, such as pediatric stroke.

Cerebral blood flow quantification in age groups

Another issue that is related to pediatric perfusion imaging is the potential error in CBF quantification using perfusion models with physiologic parameters that were derived from adults. In the single-compartment model, assuming that all of the labeled blood stays in the vasculature, perfusion errors arise mainly from the choice of two parameters: the T1 of blood (T_{1a}) and the blood brain partition coefficient of water (λ). Blood T1 in children is expected to be longer than the adult value because the blood water content is higher than in adults [51]. As a result, adopting adult blood T1 for perfusion quantification in children may lead to overestimation of CBF. Conversely, previous data suggest that the blood brain partition coefficient of water is greater in children (1.1 mL/g in neonates) [51] than in adults (0.9 mL/g), which would cause underestimation of child CBF by using the adult λ. Because the effects of λ and T_{1a} tend to be counterbalanced by each other, the adult perfusion model provides a reasonable approximation of child CBF quantification, and yields CBF measures that are comparable to values that are obtained using radioactive methods [35]. Based on simulation, there may be a slight (10%) overestimation of perfusion in neonates, but the overall error is approximately 5% across the entire age span (0–18 years). Given the sparse literature and large variability of these parameters in pediatric age groups, CBF quantification that is based on adult perfusion models seems to be a reasonable solution. Nevertheless, optimizing the specific perfusion model for pediatric populations bears considerable importance and significance in clinical diagnosis, because these parameters may vary with the pathologic state. Recent literature also suggested that the two-compartment perfusion model, which takes into account the limited water exchange (permeability) between capillary and brain tissue, may provide a more accurate perfusion estimation compared with the single-compartment model [25]. The two-compartment perfusion model involves more parameters that may vary with age, such as the permeability surface (PS) product and the T2/T2* of blood and brain tissue. The effects of the choice of these parameters on CBF measurement in children awaits further investigation.

The following sections discuss the specific applications of ASL perfusion MR imaging in pediatric neurologic disorders. These studies were performed primarily using PASL and CASL methods at 1.5 T. Although it is too soon to include high-field (3.0 T) studies (in progress) in this article, the authors believe that high-field ASL represents the future direction for pediatric perfusion imaging.

Normal development

Human brain maturation and development is incomplete at birth. Brain development is associated with changes in cellular metabolism and CBF that progress in stages through the first decade of life before trailing off and dropping to adult levels at approximately 15 years of age [35,52]. Whereas several studies have measured CBF in premature infants or infants who had critical illness [53–55], studies of normal infants and children are scarce. Only two studies have attempted to catalog normative CBF data across age groups; one used transcranial Doppler to measure CBF volumes [56], and the other analyzed SPECT scans that were performed for clinical indications (not specified) and retrospectively were found to be transient or not accompanied by CNS pathology [35]. In both studies, sample size was small and the conclusions are limited.

The authors performed PASL perfusion MR imaging on seven neurologically normal children and five healthy adults [38]. The SNR of the perfusion images, CBF along with T1, M0 were measured and compared between the two age groups. In the cohort of neurologically normal children, a 70% increase in the SNR of the ASL perfusion images and a 30% increase in the absolute CBF, compared with the adult data, were observed. The measures of ASL SNR, T1, and M0 decreased linearly with age. Fig. 6 displays the measured ASL SNR and global CBF as a function of age. Although the small sample size did not allow detailed analysis of the developmental curve of CBF, the observed ratio (1.3) of CBF in the child versus adult group was highly compatible with previous studies [35,57].

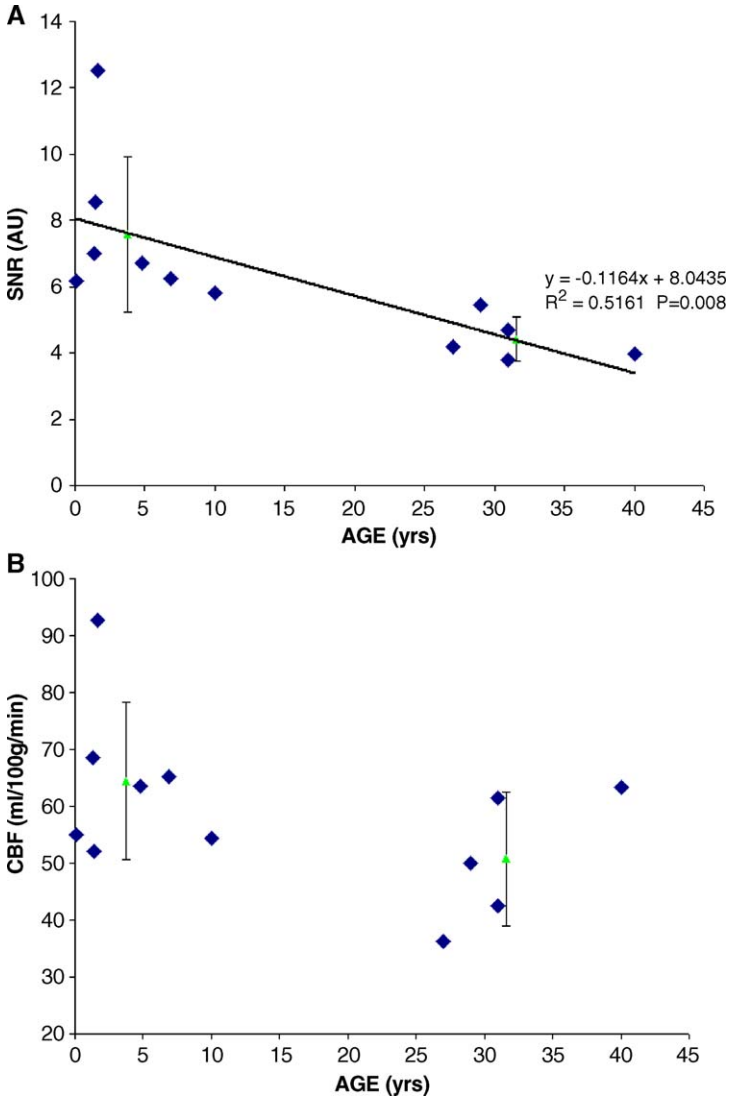

Fig. 6. Measures of whole-brain based ASL SNR (*A*) and CBF (*B*) as a function of age. ASL SNR shows a negative linear relationship with age. The triangle symbols and error bars represent the mean and SD of the CBF measurements in child and adult groups.

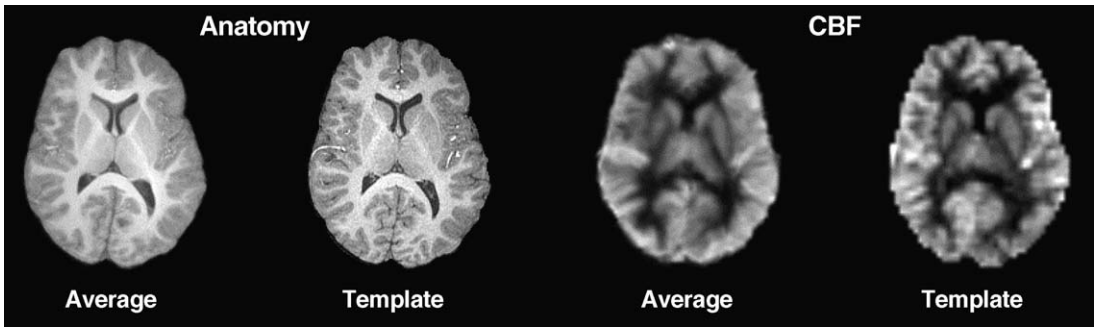

Fig. 7. Average and template anatomic and perfusion images in five normal children. Each individual's images are first normalized to the template using the HAMMER method and then averaged.

Recently, the authors also performed the AM CASL method at 3.0 T to obtain normative perfusion data of the developing brain. Because of improved image quality and whole-brain coverage, these perfusion images can be coregistered with high-resolution anatomic MR imaging that is acquired during the same scanning session. This provides the potential to construct a template or atlas of normal brain perfusion in children of different ages. Fig. 7 displays an example perfusion template that was constructed from five normal children aged 7 to 10 years. After skull stripping, the structural MR images of these children were normalized automatically using a nonlinear elastic algorithm termed HAMMER (hierarchical attribute matching mechanism for elastic registration) [58]. Perfusion images were normalized and averaged following the transformation matrix that was determined from the structural MR imaging. Compared with the statistical parametric mapping (SPM) template of brain perfusion that is based on nuclear medicine approaches, the ASL perfusion template offers improved anatomic detail and is acquired using completely noninvasive methods.

Congenital heart defects

Concurrent with the growing interest in neuroprotective strategies in the injured newborn, there has been an increasing awareness of brain injury in children who are survivors of early heart surgeries. Approximately 30,000 infants are born with congenital heart disease in the United States each year. One third of these infants have severe, complex cardiac lesions that require surgical repair in the first few months of life. Cardiac surgery for serious forms of CHDs in the neonatal period has progressed to the point where mortality is minimal and impaired neurodevelopmental outcome represents a major morbidity for survivors. After surgery, several large studies demonstrated that more than 50% of these patients develop lesions of the white matter of the brain in the form of periventricular leukomalacia (PVL) [59–61]. One study performed preoperative brain MR imaging, and demonstrated PVL in almost 20% of the infants who were tested [59]. The PVL in patients who have CHDs resembles a milder form of PVL than that which results from premature birth, and PVL in prematurity has been attributed, in part, to cerebral hypoperfusion.

Hypoplastic left heart syndrome (HLHS) is a particularly severe form of CHD that is characterized by a diminutive left ventricle and atresia, or severe hypoplasia, of the aortic valve and aorta. The left ventricle outflow obstruction that is created by the atretic aortic valve forces all systemic blood flow through the ductus arteriosus. Retrograde blood flow up the descending aorta fills the neck vessels. Other forms of complex CHD (non-HLHS), including transposition of the great arteries and tetralogy of Fallot, also necessitate corrective surgeries early in life. These forms of CHD also are dependent on an open ductus arteriosus, but the blood flow is for pulmonary, and not systemic, perfusion. With this physiology, the low-resistance pulmonary vascular bed steals blood flow in diastole. As such, whether related to reversal of blood flow in the ascending aorta or diastolic run-off, there are physiologic reasons for decreased CBF in both groups.

Because ASL does not require bolus contrast injection and no wash-out time is required, several CBF measurements can be made in a single sitting. This allows for measurements of resting CBF and CBF measurements under the condition of increased inspired carbon dioxide (CO_2). Furthermore, test–retest measurements could be made with both conditions. CO_2 is a potent cerebral arteriolar vasodilator and an equally potent pulmonary arteriolar vasoconstrictor. Increased inspired CO_2 was shown by near-infrared spectroscopy to increase mixed venous oxygenation significantly in neonates who had HLHS [62], and to increase CBF during hypothermic cardiopulmonary bypass [63,64]. Measuring the CBF response to CO_2 is a marker for physiologic reserve in the cerebrovascular bed. CO_2 reactivity (change in CBF/change in P_{CO_2}) is of interest because impaired CO_2 reactivity has been associated with poor neurodevelopmental outcome and a higher risk of death in all age groups [65,66].

The authors conducted an investigation, at 1.5 T, using PASL perfusion MR imaging to quantify preoperative CBF in 25 infants who had CHD [60], in an attempt to test the hypothesis that CBF is low and may be associated with observed PVL, and to measure cerebral vascular responsiveness to inspired CO_2. In the authors' cohort, CBF values were measured and regarded as specific risk factors for the observed preoperative structural brain abnormalities. The mean CBF value for the cohort was 19.7 ± 9.1 mL/100 g/min (representative images are presented in Fig. 8), which was much less than the normal value of 50 ± 3.4 mL/100 g/min that was reported by Chiron and colleagues [35] in term infants under conditions of conscious sedation. Lou and colleagues [53], using xenon-133 clearance methodology, studied 19 sick neonates. They demonstrated that global CBF of less than 20 mL/100 g/min was highly predictive of cerebral atrophy at autopsy or follow-up head CT. Significantly, 5 neonates (20%) in the authors' study had CBF values that were less than or equal to 10 mL/100 g/min, the level that was shown to cause moderate ischemic changes in piglets [67]. In the

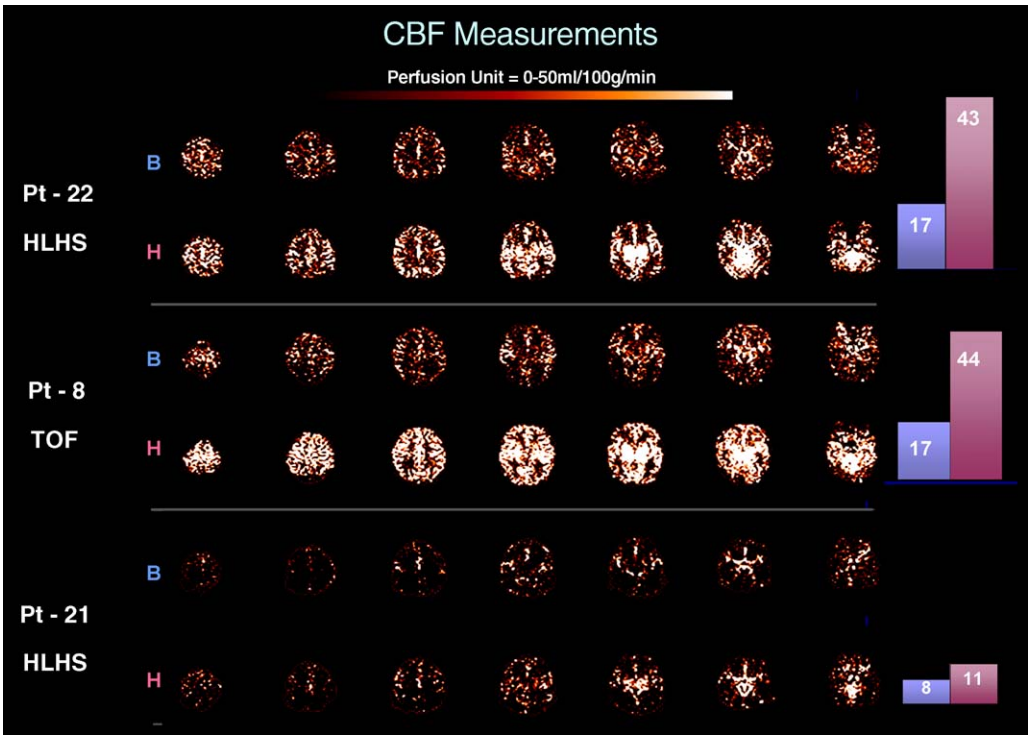

Fig. 8. Representative images from three patients (Pt-22, -8, and -21) who were enrolled in the Congenital Heart Defect Study. CBF images at baseline (B) and under hypercarbic (H) conditions are shown. The histograms at the far right are the global measurements of baseline (*blue*) and hypercarbic CBF (*red*). TOF, tetralogy of Fallot.

authors' study, baseline CBF varied directly with systolic blood pressure and inversely with hemoglobin concentration ($P \leq .001$ for both). Our observed low CBF measurements also were congruent with the study of Greeley and colleagues, which included neonates, although specific neonatal CBF values were not detailed [63,64,68]. CO_2 reactivity for the cohort averaged 0.96 ± 0.61 mL/min/100 g/mm Hg with a wide range from 0.22 to 2.17 mL/min/100 g/mm Hg. In previous pediatric studies, CO_2 reactivity of more than 2 mL/min/100 g/mm Hg was associated with survival, whereas reactivity of less than 1.0 mL/min/100 g/mm Hg was associated with death or poor neurologic outcome [65,66]. In the authors' study of 25 preoperative infants who had severe CHD, PVL occurred in 28% (7/25) and was associated with decreased baseline CBF values ($P = .05$) and lower CO_2 reactivity ($P = .02$). In addition, the neonatal perfusion images showed greater blood flow in brain stem, thalamus, basal ganglia, and sensorimotor cortex, which are in excellent agreement with a previous study that used a nuclear medicine approach [69].

Low baseline CBF measurements in our study are consistent with earlier reports of elevated preoperative white matter lactate [59], which indicates early ischemia, and is supported further by the occurrence of ischemic lesions (PVL) in more than 20% of the patients. The study suggests that the preoperative CBF levels are extraordinarily low, and in most cases, the cerebral vascular resistance is low and cannot be altered by inspired CO_2. These data draw attention to the important role of preoperative cerebral perfusion as an underrecognized preoperative risk factor for brain injury.

Pediatric stroke

Emerging neuroimaging techniques have allowed minimally invasive, rapid assessment of brain lesions in adults who have an acute stroke [70–72]. Although imaging and treatment protocols for adults who had a stroke have been well established, the same degree of attention has not been applied to children who have had a stroke. Stroke affects from 2 to 8 children per 100,000 who are younger than age 18 every year in Europe [73] and North America [74], and ranks among the top 10 causes of death in this age group [75]. Long-term motor and cognitive deficits that interfere with activities of daily life and academic performance affect 40% to 60% of survivors of childhood stroke. Studies to examine the relation of clinical symptoms at presentation with neuroimaging data are lacking.

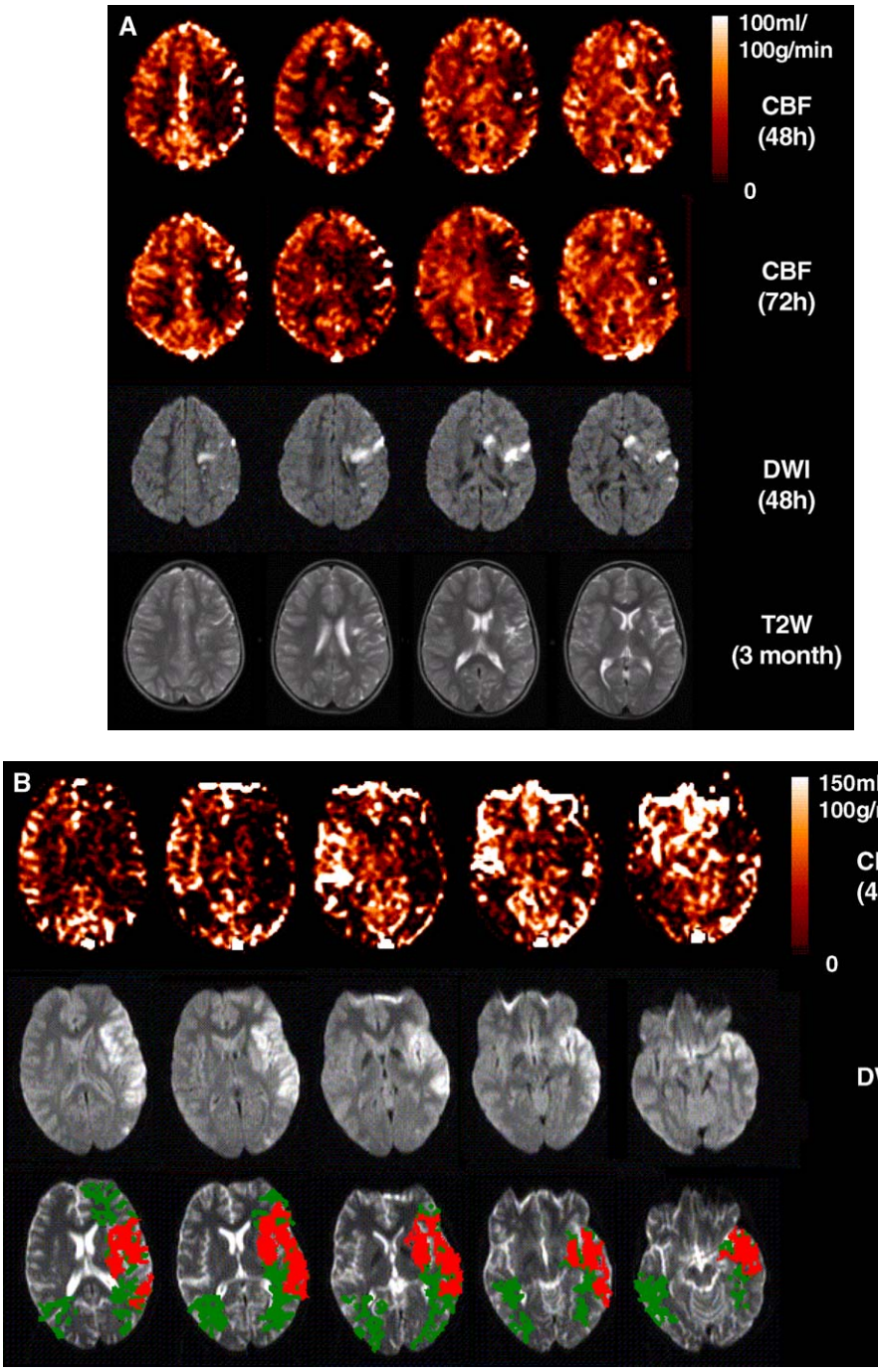

Fig. 9. (*A*) PASL perfusion MR imaging acquired at 48 hours and 72 hours from symptom onset in a 6-year-old boy who presented with Varicella vasculopathy and stroke are shown in the top two rows. Also shown are DWI (*third row*), and T2-weighted images that were taken at long-term follow-up (*bottom*). (*B*) 15-year-old boy who had HIV-associated vasculitis. CBF and diffusion images are shown in the top and second rows respectively. Overlay of perfusion (*green*) and diffusion (*red*) deficits is displayed in the bottom row.

In adult strokes, a mismatch between perfusion and diffusion defects (penumbra) has been suggested as an indicator that the untreated stroke will expand with time and is an emerging indication for therapy [76]. Therefore, the potential indications for perfusion imaging in pediatric stroke are to identify viable tissue that is at risk of infarction and to select suitable patients for thrombolytic therapy. With this background, stroke imaging protocols were constructed for the evaluation of acute (< 6 hours from symptom onset), subacute (> 6 hours from symptom onset), and chronic (> 72 hours from symptom onset) vascular changes at our institute (Children's Hospital of Philadelphia). All imaging protocols include diffusion-weighted imaging (DWI) and ASL perfusion MR imaging, among other sequences. To date, 29 cases of stroke (14 arterial ischemic strokes) have been scanned with this protocol.

Fig. 9A shows a case of pediatric ischemic stroke in a 6-year-old boy. ASL perfusion and DWIs were acquired at 48 and 72 hours after symptom onset. Regions of hypoperfusion are present in the left middle cerebral artery (MCA) territory, which is consistent with the infarct location that was detected in the DWI. The two CBF measurements with a 1-day interval are reproducible, which demonstrates the stability of the technique and its potential use in longitudinal studies to track stroke development. A mismatch between the deficits in the CBF and DWI is observed, akin to the ischemia penumbra pattern in adult stroke. When compared with follow-up T2-weighted images at 3 months, the eventual infarct did not extend beyond the initial diffusion lesion volume. Another case of hyperacute ischemic stroke (15-year-old boy) is shown in Fig. 9B. Perfusion and diffusion images were acquired within 4 hours after symptom onset. A close match between the perfusion and diffusion deficits in the left MCA territory is observed, yet perfusion images indicate reduced CBF in the posterior right MCA territory. Delayed transit effects (bright focal signal) are present in both cases, and suggest that blood flow in the affected region may be compensated through collateral blood supply. The volume of perfusion and diffusion lesions can be determined by using a semiautomatic segmentation program with human guidance [see Fig. 9B].

In addition to acute infarction, the authors also assessed the usefulness of PASL perfusion MR imaging in pediatric patients who had arteriopathies. The patients ranged in age from 3 days to 15 years, and the vascular abnormalities included moya moya, focal segmental stenosis, HIV, and congenital absence of the internal carotid arteries. Compared with DWI and T2 MR imaging sequences, ASL showed defects that matched infarct location and equaled or exceeded infarct size in all patients who had acute or chronic infarcts. In patients who had arterial stenoses without infarct on their clinical imaging, perfusion imaging demonstrated resting deficits in the arterial territory or focal intravascular signals because of a prolonged transit time [77].

Transit time estimation

Besides CBF quantification, arterial transit time from tagging region to brain tissue can be imaged using the FEAST technique. Arterial transit time in ASL methods is conceptually analogous to the time-to-peak in DSC methods. When arterial perfusion pressure decreases as a result of vasculopathy, perfusion can be maintained through reduced vascular resistance and collateral sources of blood supply until the autoregulatory capability is exhausted. Arterial transit time is more sensitive to the change in arterial perfusion pressure, and provides additional information (eg, collateral blood supply) that is not available with ASL measurement alone. Fig. 10 shows a representative data set of perfusion and transit time images of a patient (3-year-old boy) who had congenital left internal carotid artery stenosis that was indicated clinically by MR angiography (MRA). CBF images show normal global perfusion (62 mL/100 g/min) with potential transit effects in the left hemisphere. The transit time measured using FEAST is prolonged in the left hemisphere, which suggests that perfusion in these regions is maintained through collateral blood supply, and also explains the transit-related hyperintensity in the CBF images.

Silent ischemia in sickle cell disease

Children who have sickle cell disease (SCD) and who have no history of overt stroke are still at risk for brain injury that is manifested by cognitive impairment—a major source of morbidity in this population [78]. Conventional diagnostic methods, such as anatomic MR imaging, MRA, and transcranial Doppler, are not sensitive for demonstrating the extent and severity of brain injury, and may be normal in most of these children [78]. Understandably, conventional diagnostic methods do not interrogate fully the mechanisms of brain injury in SCD, which, in addition to macrocirculatory disease, consist of microcirculatory occlusion and chronic regional tissue hypoxia and acidosis [79]. Thus, there is a need for more sensitive diagnostic tools that can identify children who are at risk before the onset of brain injury.

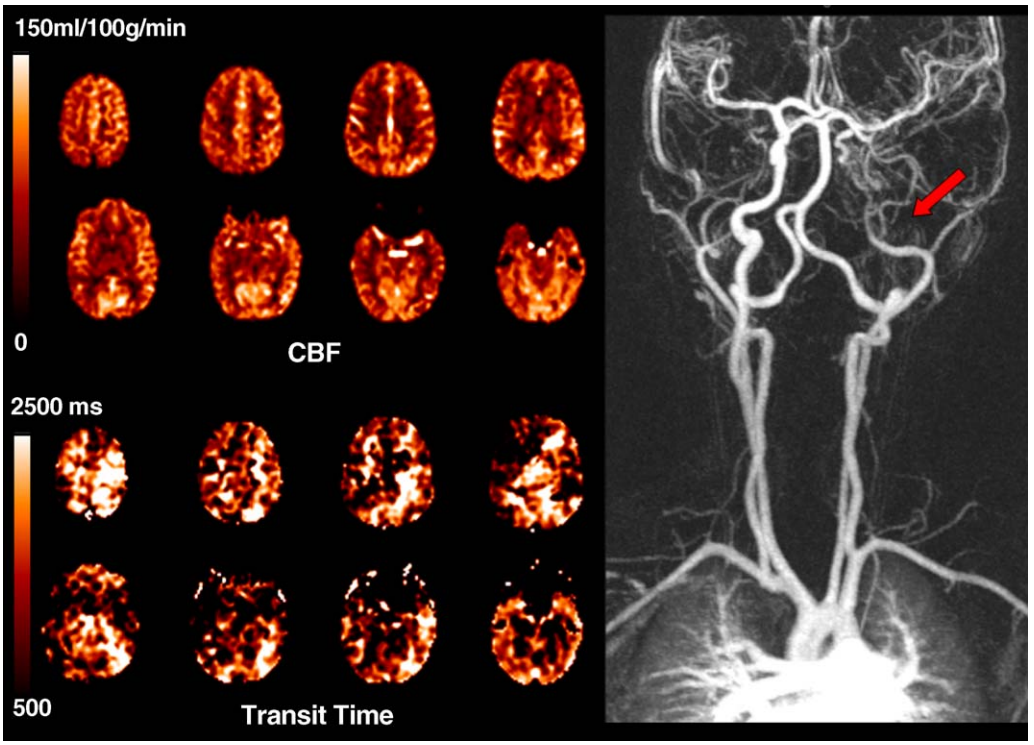

Fig. 10. Three-year-old boy who had congenital left internal carotid artery stenosis (*red arrow, top right*). CBF and FEAST transit time maps are shown in left top and bottom, respectively.

Perfusion MR imaging may provide information about the effects of small vessel disease, hemoglobin, Pa_{O_2}, and Pa_{CO_2} on brain tissue perfusion that usually is unattainable with conventional MR imaging, MRA, or transcranial Doppler sonography. CASL perfusion MR imaging was used, at 1.5 T, to assess CBF in 7 control subjects and 14 children who had SCD. Patients who had SCD had a significant increase in gray matter CBF in all cerebral arterial territories as compared with control subjects. The observed elevated baseline CBF in patients who had SCD concurred with previous studies [80,81] that used PET and xenon-enhanced CT, and was attributed, in part, to low hematocrit levels. The consequence of this chronic adaptive cerebral vasodilation is secondary depletion of the brain's reserve capacity in the face of occasional decreases in cerebral perfusion pressure; this renders children who have SCD susceptible to distal-field metabolic dysfunction, ischemia, and eventual infarction. There also was a significant decrease in baseline CBF in territories that were depicted as unaffected on conventional MR images and MRAs in 4 children who had SCD. The ability to show territorial reductions in CBF in 4 patients, underscored the potential of CASL perfusion MR imaging for further study of the effects of small vessel disease on brain tissue perfusion in SCD, although the ability of ASL perfusion imaging to identify patients who are at risk for clinical and subclinical brain infarcts and cognitive decline remains to be assessed [1].

Future directions

Perinatal hypoxic-ischemic encephalopathy

Perinatal HIE is another example where knowledge of cerebrovascular physiology could affect management strategies greatly. The prevalence of HIE has remained constant at two to nine cases per 1000 births over the past 4 decades. Therapeutic intervention in the form of selective brain cooling to reduce delayed neuronal death or programmed cell death after birth asphyxia will become possible within the next few years [82]. The report that was issued by the CoolCap Study Group found that selective brain cooling was neuroprotective in infants who had less severe abnormalities on amplitude-integrated electroencephalogram (EEG) [82]. The ultimate neurocognitive outcome of these interventions will not be known for years after birth. Neurodevelopmental testing at 1 year has poor predictive value [83], and patients with poor long-term outcome frequently are missed during testing at 12 months. For more details regarding

the epidemiology, pathophysiology, and imaging of perinatal HIE see the article by Barkovich elsewhere in this issue.

The goal of selective brain cooling in infants who are exposed to HIE is to reduce metabolic demand in neurons during the delayed energy failure that occurs 6 to 15 hours after injury [84]. Because CBF mirrors cerebral metabolism, ASL measurements of regional CBF before, during, and after selective hypothermia allow insight into the efficacy of therapy and better define optimal treatment strategies. When coregistered with anatomic MR imaging, these studies hold promise as a surrogate marker for brain injury and neurodevelopmental outcome.

Epilepsy

Epilepsy affects approximately 45,000 children each year, which results in approximately 315,000 affected children through age 14 [85]. Of these children, more than 10% do not respond to conventional medical therapies, and often are referred to a pediatric epilepsy center for possible surgical intervention. Although surgical intervention is not applicable to all refractory patients, improvements in EEG monitoring and neuroimaging are making this a possibility for more children. Therefore, localization of the seizure focus is of the utmost importance if the surgical intervention is to be successful.

At most epilepsy centers, the current standard evaluation of a child who has medically refractory extratemporal epilepsy includes high-resolution anatomic imaging (conventional or volumetric MR imaging) and EEG mapping. Assessment of tissue metabolism using SPECT [86] also is standard practice with the assumption that the epileptogenic focus is abnormal tissue that has a decreased metabolic rate and, likewise, blood flow between seizures. Coregistration of these data are accomplished primarily by visual inspection. ASL perfusion MR imaging has been used successfully to identify abnormal hippocampal tissue in adults who have temporal lobe epilepsy [87]. It is noninvasive and allows for immediate correlation and coregistration of CBF with volumetric conventional MR imaging in one sitting.

Childhood neoplasm

Childhood neoplasm is another area in which the understanding of cerebral hemodynamics may contribute to the diagnosis and prognosis of disease. Using DSC MR imaging, it was shown in adult [88,89] and pediatric [90,91] brain tumors that measures of higher blood flow and blood volume are associated with advanced tumor grade. Recently, similar results were demonstrated using PASL and CASL methods [92–94]; however, these observations have not been replicated in childhood brain tumors. The article by Young-Poussaint elsewhere in this issue provides further information on advanced imaging of pediatric cerebral neoplasms.

The use of DSC and ASL may have complementary roles in perfusion imaging of brain tumor. The microvasculature in brain tumor may be characterized by angiogenesis changes in capillary permeability, and volume. Because ASL methods use arterial blood water as a freely diffusible tracer (actually there is limited exchange rate of water across the brain–blood barrier), perfusion measurement of tumor using ASL is much less sensitive to changes in permeability and capillary blood volume than are DSC methods. Conversely, although DSC MR imaging is difficult to use for the absolute quantification of tumor blood flow, it can be used to image permeability changes in brain tumor because of its sensitivity to impaired function of the brain–blood barrier. The authors' experience in adult brain tumor imaging supports the above point [94]. Nevertheless, because of their capability for absolute quantification and completely noninvasive measurement, ASL methods provide an important option for hemodynamic neuroimaging of brain tumors, especially in children.

The effect of sedation is another important factor in pediatric perfusion imaging using ASL. The effects of sedatives on childhood brain metabolism, including CBF, CBV, and oxygen consumption, are complicated and not well understood. A general trend of suppressed cerebral metabolism has been reported during anesthesia in humans and animals [95,96]. For relative CBF/CBV measures using DSC MR imaging, the sedation effect is small because of its focus on regional change in hemodynamics. For ASL perfusion measurements, however, the sedation effect has to be taken into account, especially for multiple scans in longitudinal studies. The type and dosage of sedatives for each scan need to be recorded and considered for final analysis. ASL methods also may offer a practical way to study the cerebral effects of different procedures of sedation and anesthesia.

Functional MR imaging

The hemodynamic response, based on the blood oxygenation level–dependent (BOLD) contrast, may be dramatically different in children compared with adults, and it affects the interpretation of results of cognitive neuroimaging studies on children of different ages [97]. ASL perfusion MR imaging may provide a noninvasive means to elucidate the biophysical mechanism that underlies altered hemodynamic response in children. For example, it was reported that sedated children responded to visual stimulation with a decrease in perfusion

and BOLD signals [98]. Although these observations are not understood fully, the combination of absolute physiologic information that is obtained with ASL and relative hemodynamic changes probed with BOLD holds great potential in developmental neuroscience.

Summary

During the past decade, technical developments of ASL perfusion MR imaging have brought this technique from feasibility studies to the frontier of clinical usage. Pediatric perfusion imaging, given its unique advantages of increased blood flow and water content of the childhood brain, may offer the most promising clinical field where ASL perfusion MR imaging will eventually become a practical tool influencing patient care and management. With feasibility already demonstrated and valuable clinical information obtained in several pediatric neurologic disorders, more exploratory and validation studies need to be performed in other childhood diseases using more advanced techniques. Because we know so little about hemodynamic variations in various brain disorders in children, ASL perfusion MR imaging is bound to provide ground-breaking information in many fields of pediatric neuroimaging.

References

[1] Oguz KK, Golay X, Pizzini FB, et al. Sickle cell disease: continuous arterial spin-labeling perfusion MR imaging in children. Radiology 2003; 227(2):567–74.
[2] Johnson NA, Jahng GH, Weiner MW, et al. Pattern of cerebral hypoperfusion in Alzheimer disease and mild cognitive impairment measured with arterial spin-labeling MR imaging: initial experience. Radiology 2005;234(3):851–9.
[3] Hillis AE, Wityk RJ, Beauchamp NJ, et al. Perfusion-weighted MRI as a marker of response to treatment in acute and subacute stroke. Neuroradiology 2004;46(1):31–9.
[4] Grueneich R, Ris MD, Ball W, et al. Relationship of structural magnetic resonance imaging, magnetic resonance perfusion, and other disease factors to neuropsychological outcome in sickle cell disease. J Pediatr Psychol 2004;29(2):83–92.
[5] Ball Jr WS, Holland SK. Perfusion imaging in the pediatric patient. Magn Reson Imaging Clin N Am 2001;9(1):207–30.
[6] Huisman TA, Sorensen AG. Perfusion-weighted magnetic resonance imaging of the brain: techniques and application in children. Eur Radiol 2004;14(1):59–72.
[7] Ostergaard L, Weisskoff RM, Chesler DA, et al. High-resolution measurement of cerebral blood flow using intravascular tracer bolus passages. Part I: Mathematical approach and statistical analysis. Magn Reson Med 1996;36(5):715–25.
[8] Detre JA, Alsop DC. Perfusion fMRI with arterial spin labeling (ASL). In: Moonen CTW, Bandettini PA, editors. Functional MRI. Heidelberg (Germany): Springer-Verlag; 1999. p. 47–62.
[9] Wong EC. Potential and pitfalls of arterial spin labeling based perfusion imaging techniques for MRI. In: Moonen CTW, Bandettini PA, editors. Functional MRI. Heidelberg (Germany): Springer-Verlag; 1999. p. 63–9.
[10] Detre JA, Zhang W, Roberts DA, et al. Tissue specific perfusion imaging using arterial spin labeling. NMR Biomed 1994;7:75–82.
[11] Yang Y, Engelien W, Xu S, et al. Transit time, trailing time, and cerebral blood flow during brain activation: measurement using multislice, pulsed spin-labeling perfusion imaging. Magn Reson Med 2000;44(5):680–5.
[12] Ye FQ, Mattay VS, Jezzard P, et al. Correction for vascular artifacts in cerebral blood flow values measured by using arterial spin tagging techniques. Magn Reson Med 1997;37(2):226–35.
[13] Gonzalez-At JB, Alsop DC, Detre JA. Perfusion and transit time changes during task activation determined with steady-state arterial spin labeling. Magn Reson Med 2000;43:739–46.
[14] Alsop DC, Detre JA. Reduced transit-time sensitivity in noninvasive magnetic resonance imaging of human cerebral blood flow. J Cereb Blood Flow Metab 1996;16:1236–49.
[15] Wong EC, Buxton RB, Frank LR. Quantitative imaging of perfusion using a single subtraction (QUIPSS and QUIPSS II). Magn Reson Med 1998;39(5):702–8.
[16] Alsop DC, Detre JA. Multisection cerebral blood flow MR imaging with continuous arterial spin labeling. Radiology 1998;208:410–6.
[17] McLaughlin AC, Ye FQ, Pekar JJ, et al. Effect of magnetization transfer on the measurement of cerebral blood flow using steady-state arterial spin tagging approaches: a theoretical investigation. Magn Reson Med 1997;37(4):501–10.
[18] Wang J, Alsop DC, Li L, et al. Comparison of quantitative perfusion imaging using arterial spin labeling at 1.5 and 4.0 Tesla. Magn Reson Med 2002;48(2):242–54.
[19] Wong EC, Buxton RB, Frank LR. A theoretical and experimental comparison of continuous and pulsed arterial spin labeling techniques for quantitative perfusion imaging. Magn Reson Med 1998;40(3):348–55.
[20] Roberts DA, Detre JA, Bolinger L, et al. Quantitative magnetic resonance imaging of human brain perfusion at 1.5 T using steady-state inversion of arterial water. Proc Natl Acad Sci USA 1994;91:33–7.
[21] Utting JF, Thomas DL, Gadian DG, et al. Velocity-driven adiabatic fast passage for arterial spin labeling: results from a computer model. Magn Reson Med 2003;49(2):398–401.
[22] Maccotta L, Detre JA, Alsop DC. The efficiency

of adiabatic inversion for perfusion imaging by arterial spin labeling. NMR Biomed 1997;10: 216–21.
[23] Ewing JR, Cao Y, Fenstermacher J. Single-coil arterial spin-tagging for estimating cerebral blood flow as viewed from the capillary: relative contributions of intra- and extravascular signal. Magn Reson Med 2001;46:465–75.
[24] Parkes LM, Tofts PS. Improved accuracy of human cerebral blood perfusion measurements using arterial spin labeling: accounting for capillary water permeability. Magn Reson Med 2002; 48(1):27–41.
[25] St Lawrence KS, Wang J. Effects of the apparent transverse relaxation time on cerebral blood flow measurements obtained by arterial spin labeling. Magn Reson Med 2005;53(2):425–33.
[26] Ye FQ, Berman KF, Ellmore T, et al. $H_{(2)}^{(15)}O$ PET validation of steady-state arterial spin tagging cerebral blood flow measurements in humans. Magn Reson Med 2000;44(3):450–6.
[27] Siewert B, Schlaug G, Edelman RR, et al. Comparison of EPISTAR and T2*-weighted gadolinium-enhanced perfusion imaging in patients with acute cerebral ischemia. Neurology 1997;48: 673–9.
[28] Wolf RL, Alsop DC, McGarvey ML, et al. Susceptibility contrast and arterial spin labeled perfusion MRI in cerebrovascular disease. J Neuroimaging 2003;13(1):17–27.
[29] Floyd TF, Ratcliffe SJ, Wang J, et al. Precision of the CASL-perfusion MRI technique: global and regional cerebral blood flow within vascular territories at one hour and one week. J Magn Reson Imaging 2003;18:649–55.
[30] Wang J, Aguirre GK, Kimberg DY, et al. Arterial spin labeling perfusion fMRI with very low task frequency. Magn Reson Med 2003;49:796–802.
[31] Detre JA, Alsop DC, Vives LR, et al. Noninvasive MRI evaluation of cerebral blood flow in cerebrovascular disease. Neurology 1998;50: 633–41.
[32] Alsop DC, Detre JA, Grossman M. Assessment of cerebral blood flow in Alzheimer's disease by spin-labeled magnetic resonance imaging. Ann Neurol 2000;47:93–100.
[33] Chalela JA, Alsop DC, Gonzalez-Atavalez JB, et al. Magnetic resonance perfusion imaging in acute ischemic stroke using continuous arterial spin labeling. Stroke 2000;31:680–7.
[34] Detre JA, Samuels OB, Alsop DC, et al. Noninvasive MRI evaluation of CBF with acetazolamide challenge in patients with cerebrovascular stenosis. J Magn Reson Imaging 1999;10:870–5.
[35] Chiron C, Raynaud C, Maziere B, et al. Changes in regional cerebral blood flow during brain maturation in children and adolescents. J Nucl Med 1992;33(5):696–703.
[36] Dobbing J, Sands J. Quantitative growth and development of human brain. Arch Dis Child 1973; 48(10):757–67.
[37] Schoning M, Staab M, Walter J, et al. Transcranial color duplex sonography in childhood and adolescence. Age dependence of flow velocities and waveform parameters. Stroke 1993;24(9): 1305–9.
[38] Wang J, Licht DJ, Jahng GH, et al. Pediatric perfusion imaging using pulsed arterial spin labeling. J Magn Reson Imaging 2003;18(4):404–13.
[39] Kim SG. Quantification of relative cerebral blood flow change by flow-sensitive alternating inversion recovery (FAIR) technique: application to functional mapping. Magn Reson Med 1995; 34(3):293–301.
[40] van der Knaap MS, Valk J. MR imaging of the various stages of normal myelination during the first year of life. Neuroradiology 1990; 31(6):459–70.
[41] Wang J, Licht D, Silvestre DW, et al. Why perfusion in neonates with congenital heart defects is negative? Technical issues related to pulsed arterial spin labeling. Magn Res Imag 2005, in press.
[42] Haacke EM, Brown RW, Thompson MR, et al. Magnetic resonance imaging. New York: John Wiley & Sons, Inc.; 1999.
[43] Collins CM, Smith MB. Signal-to-noise ratio and absorbed power as functions of main magnetic field strength, and definition of "90" RF pulse for the head in the birdcage coil. Magn Rason Med 2001;45:684–91.
[44] Yongbi MN, Fera F, Yang Y, et al. Pulsed arterial spin labeling: comparison of multisection baseline and functional MR imaging perfusion signal at 1.5 and 3.0 T: initial results in six subjects. Radiology 2002;222(2):569–75.
[45] Talagala SL, Ye FQ, Ledden PJ, et al. Whole-brain 3D perfusion MRI at 3.0 T using CASL with a separate labeling coil. Magn Reson Med 2004; 52(1):131–40.
[46] Zaharchuk G, Ledden PJ, Kwong KK, et al. Multislice perfusion and perfusion territory imaging in humans with separate label and image coils. Magn Reson Med 1999;41(6):1093–8.
[47] Alsop DC, Detre JA. Multisection cerebral blood flow MR imaging with continuous arterial spin labeling. Radiology 1998;208(2):410–6.
[48] Wang J, Zhang Y, Wolf RL, et al. Amplitude-modulated continuous arterial spin-labeling 3.0-T perfusion MR imaging with a single coil: feasibility study. Radiology 2005;235(1):218–28.
[49] Wang J, Alsop DC, Song HK, et al. Arterial transit time imaging with flow encoding arterial spin tagging (FEAST). Magn Reson Med 2003;50(3): 599–607.
[50] Derdeyn CP, Grubb Jr RL, Powers WJ. Cerebral hemodynamic impairment: methods of measurement and association with stroke risk. Neurology 1999;53(2):251–9.
[51] Herscovitch P, Raichle ME. What is the correct value for the brain–blood partition coefficient for water? J Cereb Blood Flow Metab 1985;5(1): 65–9.
[52] Epstein HT. Stages of increased cerebral blood

flow accompany stages of rapid brain growth. Brain Dev 1999;21(8):535–9.
[53] Lou HC, Skov H, Pedersen H. Low cerebral blood flow: a risk factor in the neonate. J Pediatr 1979; 95(4):606–9.
[54] Greisen G. Cerebral blood flow and energy metabolism in the newborn. Clin Perinatol 1997; 24(3):531–46.
[55] Greeley WJ, Ungerleider RM, Kern FH, et al. Effects of cardiopulmonary bypass on cerebral blood flow in neonates, infants, and children. Circulation 1989;80(3 Pt 1):I209–15.
[56] Schoning M, Hartig B. Age dependence of total cerebral blood flow volume from childhood to adulthood. J Cereb Blood Flow Metab 1996; 16(5):827–33.
[57] Takahashi T, Shirane R, Sato S, et al. Developmental changes of cerebral blood flow and oxygen metabolism in children. AJNR Am J Neuroradiol 1999;20(5):917–22.
[58] Shen D, Davatzikos C. Very high-resolution morphometry using mass-preserving deformations and HAMMER elastic registration. Neuroimage 2003;18(1):28–41.
[59] Mahle WT, Tavani F, Zimmerman RA, et al. An MRI study of neurological injury before and after congenital heart surgery. Circulation 2002; 106(12 Suppl 1):I109–14.
[60] Licht DJ, Wang J, Silvestre DW, et al. Preoperative cerebral blood flow is diminished in neonates with severe congenital heart defects. J Thorac Cardiovasc Surg 2004;128(6):841–9.
[61] Galli KK, Zimmerman RA, Jarvik GP, et al. Periventricular leukomalacia is common after neonatal cardiac surgery. J Thorac Cardiovasc Surg 2004;127(3):692–704.
[62] Tabbutt S, Ramamoorthy C, Montenegro LM, et al. Impact of inspired gas mixtures on preoperative infants with hypoplastic left heart syndrome during controlled ventilation. Circulation 2001;104(12 Suppl 1):I159–64.
[63] Stockwell JA, Goldstein RF, Ungerleider RM, et al. Cerebral blood flow and carbon dioxide reactivity in neonates during venoarterial extracorporeal life support. Crit Care Med 1996; 24(1):155–62.
[64] Kern FH, Ungerleider RM, Quill TJ, et al. Cerebral blood flow response to changes in arterial carbon dioxide tension during hypothermic cardiopulmonary bypass in children. J Thorac Cardiovasc Surg 1991;101(4):618–22.
[65] Ashwal S, Stringer W, Tomasi L, et al. Cerebral blood flow and carbon dioxide reactivity in children with bacterial meningitis. J Pediatr 1990; 117(4):523–30.
[66] Ashwal S, Perkin RM, Thompson JR, et al. CBF and CBF/PCO2 reactivity in childhood strangulation. Pediatr Neurol 1991;7(5):369–74.
[67] Ichord RN, Kirsch JR, Helfaer MA, et al. Age-related differences in recovery of blood flow and metabolism after cerebral ischemia in swine. Stroke 1991;22(5):626–34.
[68] Greeley WJ, Kern FH, Ungerleider RM, et al. The effect of hypothermic cardiopulmonary bypass and total circulatory arrest on cerebral metabolism in neonates, infants, and children. J Thorac Cardiovasc Surg 1991;101(5):783–94.
[69] Chugani HT. A critical period of brain development: studies of cerebral glucose utilization with PET. Prev Med 1998;27(2):184–8.
[70] Singer OC, Du Mesnil De Rochemont R, et al. Early functional recovery and the fate of the diffusion/perfusion mismatch in patients with proximal middle cerebral artery occlusion. Cerebrovasc Dis 2004;17(1):13–20.
[71] Chalela JA, Kang DW, Luby M, et al. Early magnetic resonance imaging findings in patients receiving tissue plasminogen activator predict outcome: insights into the pathophysiology of acute stroke in the thrombolysis era. Ann Neurol 2004;55(1):105–12.
[72] Chalela JA, Ezzeddine M, Latour L, et al. Reversal of perfusion and diffusion abnormalities after intravenous thrombolysis for a lacunar infarction. J Neuroimaging 2003;13(2):152–4.
[73] Ganesan V, Prengler M, McShane MA, et al. Investigation of risk factors in children with arterial ischemic stroke. Ann Neurol 2003;53(2):167–73.
[74] Fullerton HJ, Wu YW, Zhao S, et al. Risk of stroke in children: ethnic and gender disparities. Neurology 2003;61(2):189–94.
[75] Fullerton HJ, Chetkovich DM, Wu YW, et al. Deaths from stroke in US children, 1979 to 1998. Neurology 2002;59(1):34–9.
[76] Baird AE, Benfield A, Schlaug G, et al. Enlargement of human cerebral ischemic lesion volumes measured by diffusion-weighted magnetic resonance imaging. Ann Neurol 1997;41(5):581–9.
[77] Shellhaas DW, Silvestre DW, Wang J, et al. Perfusion magnetic resonance imaging in childhood central nervous system vasculopathy and stroke. Ann Neurol 2004;56(S8):S92.
[78] Wang W, Enos L, Gallagher D, et al. Neuropsychologic performance in school-aged children with sickle cell disease: a report from the Cooperative Study of Sickle Cell Disease. J Pediatr 2001;139(3):391–7.
[79] Kaul DK, Nagel RL. Sickle cell vasoocclusion: many issues and some answers. Experientia 1993;49(1): 5–15.
[80] Powars DR, Conti PS, Wong WY, et al. Cerebral vasculopathy in sickle cell anemia: diagnostic contribution of positron emission tomography. Blood 1999;93(1):71–9.
[81] Prohovnik I, Pavlakis SG, Piomelli S, et al. Cerebral hyperemia, stroke, and transfusion in sickle cell disease. Neurology 1989;39(3):344–8.
[82] Gluckman PD, Wyatt JS, Azzopardi D, et al. Selective head cooling with mild systemic hypothermia after neonatal encephalopathy: multicentre randomised trial. Lancet 2005;365(9460): 663–70.
[83] McGrath E, Wypij D, Rappaport LA, et al. Prediction of IQ and achievement at age 8 years

from neurodevelopmental status at age 1 year in children with D-transposition of the great arteries. Pediatrics 2004;114(5):e572–6.
[84] Azzopardi D, Wyatt JS, Cady EB, et al. Prognosis of newborn infants with hypoxic-ischemic brain injury assessed by phosphorus magnetic resonance spectroscopy. Pediatr Res 1989;25(5): 445–51.
[85] Epilepsy: a report to the nation. Landover (MD): Epilepsy Foundation of America; 1999.
[86] Wu X. [Brain SPECT, CT and EEG in 45 cases of epilepsy during the intermission]. Zhonghua Shen Jing Jing Shen Ke Za Zhi 1991;24(1):6–60.
[87] Wolf RL, Alsop DC, Levy-Reis I, et al. Detection of mesial temporal lobe hypoperfusion in patients with temporal lobe epilepsy by use of arterial spin labeled perfusion MR imaging. AJNR Am J Neuroradiol 2001;22(7):1334–41.
[88] Law M, Yang S, Wang H, et al. Glioma grading: sensitivity, specificity, and predictive values of perfusion MR imaging and proton MR spectroscopic imaging compared with conventional MR imaging. AJNR Am J Neuroradiol 2003;24(10): 1989–98.
[89] Law M, Yang S, Babb JS, et al. Comparison of cerebral blood volume and vascular permeability from dynamic susceptibility contrast-enhanced perfusion MR imaging with glioma grade. AJNR Am J Neuroradiol 2004;25(5):746–55.
[90] Tzika AA, Astrakas LG, Zarifi MK, et al. Spectroscopic and perfusion magnetic resonance imaging predictors of progression in pediatric brain tumors. Cancer 2004;100(6):1246–56.
[91] Chang YW, Yoon HK, Shin HJ, et al. MR imaging of glioblastoma in children: usefulness of diffusion/perfusion-weighted MRI and MR spectroscopy. Pediatr Radiol 2003;33:836–42.
[92] Weber MA, Gunther M, Lichy MP, et al. Comparison of arterial spin-labeling techniques and dynamic susceptibility-weighted contrast-enhanced MRI in perfusion imaging of normal brain tissue. Invest Radiol 2003;38(11):712–8.
[93] Silva AC, Kim SG, Garwood M. Imaging blood flow in brain tumors using arterial spin labeling. Magn Reson Med 2000;44(2):169–73.
[94] Wolf RL, Wang J, Wang S, et al. Grading of CNS neoplasms using continuous arterial spin labeled perfusion MR. J Magn Reson Imaging 2005;22: 475–82.
[95] Theodore WH. The role of fluorodeoxyglucose-positron emission tomography in the evaluation of seizure disorders. Semin Neurol 1989;9(4): 301–6.
[96] Todd MM, Weeks J. Comparative effects of propofol, pentobarbital, and isoflurane on cerebral blood flow and blood volume. J Neurosurg Anesthesiol 1996;8(4):296–303.
[97] Gaillard WD, Grandin CB, Xu B. Developmental aspects of pediatric fMRI: considerations for image acquisition, analysis, and interpretation. Neuroimage 2001;13(2):239–49.
[98] Born AP, Rostrup E, Miranda MJ, et al. Visual cortex reactivity in sedated children examined with perfusion MRI (FAIR). Magn Reson Imaging 2002;20(2):199–205.